GEOPHYSICAL RESEARCH LETTERS, VOL. 37, L07808, doi:10.1029/2010GL042691, 2010

Impact of cloud-radiative processes on hurricane track

Robert G. Fovell,[1] Kristen L. Corbosiero,[1] Axel Seifert,[2] and Kuo-Nan Liou[1]

Received 26 January 2010; accepted 9 March 2010; published 14 April 2010.

[1] Idealized simulations of tropical cyclones suggest that previously established motion sensitivity to cloud microphysical processes may emerge through cloud-radiative feedback. When commonly employed radiation parameterizations and absorption treatments are used, microphysical schemes generate a variety of tracks, influenced by different, scheme-dependent convective heating patterns and magnitudes. However, these variations nearly vanish when cloud-radiative feedback is neglected, with storms becoming stronger and more compact. This study strongly motivates further research with respect to how condensation particles influence radiative processes and thus storm dynamics and thermodynamics. **Citation:** Fovell, R. G., K. L. Corbosiero, A. Seifert, and K.-N. Liou (2010), Impact of cloud-radiative processes on hurricane track, *Geophys. Res. Lett.*, *37*, L07808, doi:10.1029/2010GL042691.

1. Introduction

[2] Atlantic tropical cyclone (TC) track forecasts have been steadily improving. The National Hurricane Center's (NHC) website reports that average position errors at 24 and 48 h lead times were roughly 90 and 180 km in recent years. Yet, track forecasts simulated by numerical models can exhibit track sensitivities of this magnitude in response to model physics variations, such as microphysics parameterizations (MPs) and cumulus schemes. *Fovell and Su* [2007, hereafter Paper 1] showed that cloud processes could materially influence storm motion over periods as short as two days.

[3] In a higher resolution, idealized experiment, *Fovell et al.* [2009, hereafter Paper 2] demonstrated that MP schemes tend to generate different storm structures, particularly with regard to the outer wind strength located several hundred km from the center. *Fiorino and Elsberry* [1989, hereafter FE] showed these winds influence motion owing to planetary vorticity advection, the "beta effect." As explained by *Holland* [1983] and *Chan and Williams* [1987], "beta gyres" become established that impart a generally northwestward "ventilation flow" across typical Northern Hemisphere vortices. FE's storms slowed and shifted direction from northwestward to northward as the outer wind strength diminished, and Paper 2 revealed that manipulating microphysics could alter these winds, and thus influence the storm track via differential beta drift.

[4] This study extends Paper 2 by placing primary emphasis on *cloud-radiative feedback* (CRF), in which condensation particles influence the absorption and emission of longwave (LW) and shortwave (SW) radiation. We demonstrate that MP-related differences emerge primarily through CRF. This has important implications not only for track forecasting but also for further model development priorities.

2. Model

[5] As in Papers 1 and 2, an aquaplanet version of the Weather Research and Forecasting (WRF) v.2.2.1 model was used, incorporating *Jordan*'s [1958] hurricane season sounding and a fixed (29°C) sea-surface temperature, the YSU boundary layer, and the RRTM and *Dudhia*'s [1989] radiation packages. Inserting a synoptic-scale warm bubble into an initially calm, horizontally homogeneous environment and integrating for a 1 day spin-up period created the coherent TC used as the initial state for simulations extending a further 72 h. The Kessler (K), Lin-Farley-Orville (L), and WRF single-moment 3-class (W) microphysics schemes were again examined. Kessler is an ice-free scheme, while W and L incorporate two and three classes of ice, respectively. L's three frozen classes are free-floating ice crystals, low density snow aggregates and graupel.

[6] Paper 2 utilized three telescoping nests down to 3 km horizontal grid spacing, but as the results indicated potential sensitivity to storm structure at radii that might extend beyond the inner fine grid, a single 2700 km square domain at 4 km resolution was used herein. No important impacts were noted. The model top was raised to the 10 mb level, another minor alteration. More importantly, Papers 1 and 2 used a 40% relative humidity (RH) above 400 mb, the highest level reported by *Jordan* [1958]. In this experiment, the RH was fixed at 40% in the 400–200 mb layer, consistent with that of *Dunion and Marron* [2008], but set to 0 farther aloft. This altered ice production in the L scheme, influencing its track. This study adds the WRF single moment 6-class (W6) scheme, as well as two versions (S_1 and S_2) of *Seifert and Beheng*'s [2006] double-moment parameterization that differ with respect to ice to snow conversion.

[7] As further development took place over the 48 h following the spin-up period, analyses herein focus on the final 24 h, employing vortex-following compositing to extract symmetric and asymmetric components. All fields are averaged through this final period, unless indicated otherwise. For CRF-off simulations (e.g., L*), radiation physics was included but condensation particles were not permitted any influence on LW or SW radiation.

3. Results

[8] Figure 1a presents model TC tracks over a period of 72 h beyond the spin-up period for the CRF-on cases. As in the prior studies, the K storm moved swiftly to the north-

[1]Department of Atmospheric and Oceanic Sciences, University of California, Los Angeles, California, USA.
[2]German Weather Service, Offenbach, Germany.

0094-8276/10/2010GL042691

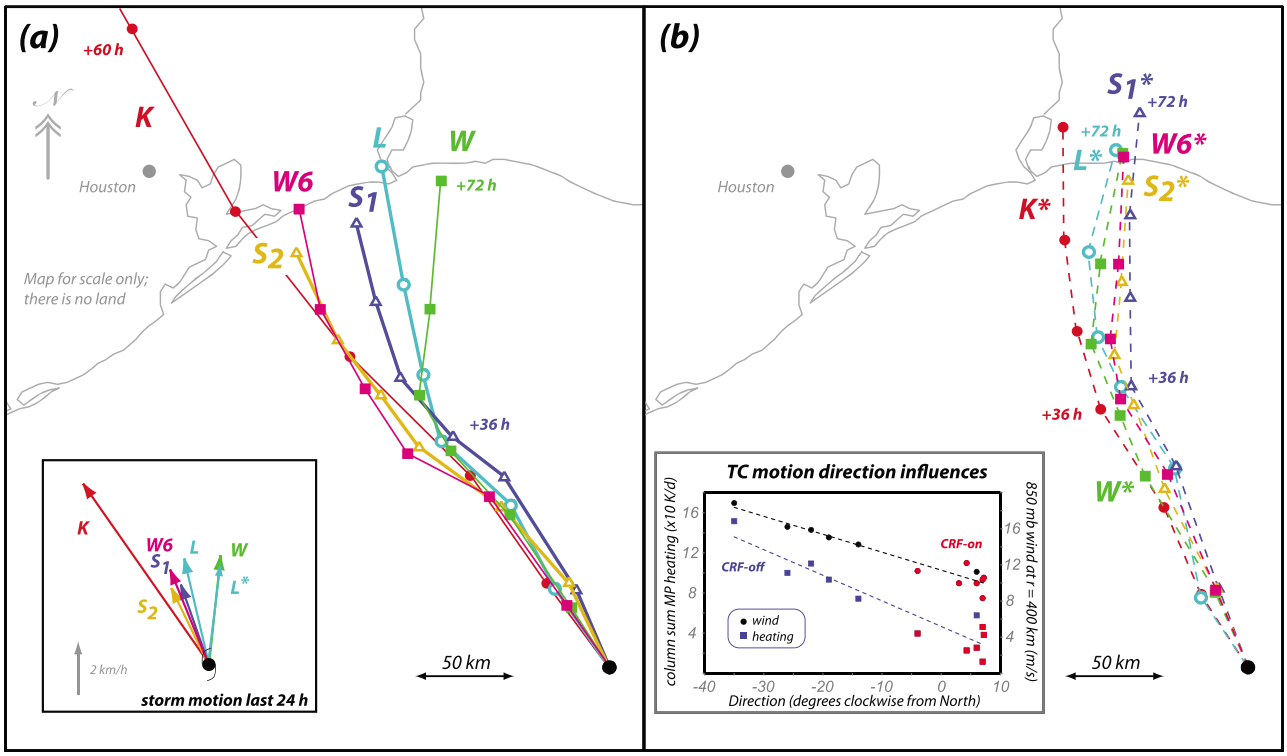

Figure 1. Twelve hourly cyclone positions over 72 h for Kessler (K), LFO (L), WSM3 (W), WSM6 (W6), and two Seifert-Beheng (S_1 and S_2) simulations with CRF (a) on and (b) off. The 72 h K position is beyond the subdomain depicted. U.S. Gulf Coast segment included for scale; the model has no land. Inset (Figure 1a): storm motion vectors for the 48–72 h period. Inset (Figure 1b): motion relative to North versus symmetric 850 mb winds at radius r = 400 km from the eye and column sum microphysics heating averaged through $200 \leq r \leq 400$ km, and least squares fits.

west, while W turned northward after 36 h and L tracked in between. The L track has been shifted eastward relative to its Paper 2 counterpart, influenced by the reduced upper-level humidity. The W6 and two Seifert tracks parallel K's, although at about half the speed.

[9] Taken together, the six storms could represent a "landfall" span of about 115 km after 3 days, mainly resulting from directional variations that appear after about 36 h rather than speed differences. Neglecting K, again the group's outlier, TC speed during the final 24 h varied little among the runs (4.1 ± 0.4 km/h). However, the directions ranged between −26 and 8 degrees relative to north, a span of 34 degrees (Figure 1a, inset). If started from a common point using mature period motion characteristics, the S_2-L cyclone separation would become 82.5 km after a single day, and storms S_2 and W would be 149.5 km apart. These values are comparable to the recent average forecast position errors cited above.

[10] Curiously, the microphysical sensitivity *nearly vanishes when CRF is neglected* (Figure 1b). The MP schemes, even K, produced very similar tracks, all turning northward after 36 h. The relationship between the 850 mb symmetric wind component at 400 km from the storm center and the storm direction relative to north (Figure 1b, inset) reveals that CRF-off storms had weaker outer winds, which is significantly correlated (R^2 = 0.95) with a more northward translation. The CRF-off TCs also generated less diabatic heating in the 200–400 km radial annulus, also well-correlated (R^2 = 0.88) with motion direction (same inset). *Wang* [2009] identified heating in the outer rainbands as a principal factor influencing the azimuthally symmetric structure of TCs, and Paper 2 demonstrated substantial wind and track sensitivity to the manipulation of convective activity in that region.

[11] It is also revealing to more directly inspect storm asymmetries that have been linked to TC motion. The CRF-on cases present a variety of vertical velocity patterns (Figure 2): weak and symmetric for K (Figure 2a); stronger ascent concentrated in the SE quadrant for W6 (Figure 2b) and S_2 (not shown); and a rotation to east and northeast for S_1, L (Figures 2c and 2d) and W (not shown). In contrast, the CRF-off storms (Figures 2e–2h) are strikingly similar, with relatively intense ascent located in the northeast sector and closer to the center. The prominent updraft asymmetry in these cases is likely due to vertical shear associated with the beta effect [cf. *Bender*, 1997], as the ventilation flow weakens with height in a warm-core vortex. Observations and theory [e.g., *Frank and Ritchie*, 1999; *Corbosiero and Molinari*, 2002] confirm that convection tends to be concentrated on the downshear and downshear-left flanks. CRF appears to weaken the updrafts and the asymmetry; this proceeds differently among the MPs, yielding the CRF-on experiment's track variation.

[12] The potential vorticity (PV) tendency equation has been shown to skillfully identify contributions to TC motion [e.g., *Wu and Wang*, 2000, 2001, hereafter WW]. The

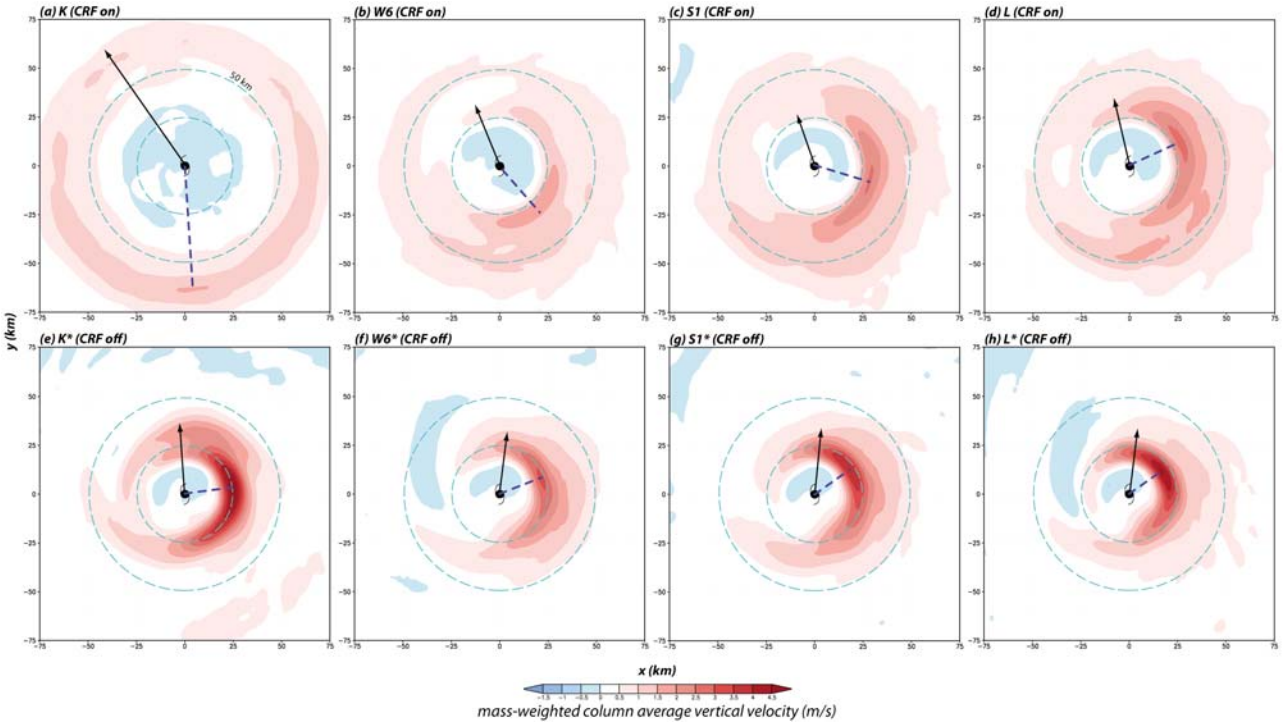

Figure 2. Vortex-following composite fields of surface-12 km layer mass-weighted mean vertical velocity, averaged over the final 24 h in a 150 km square region, for schemes K, W6, S1 and L, (a–d) with and (e–g) without CRF. Vectors represent storm motion and dashed lines point towards the largest ascent.

inviscid PV tendency (*PVT*) reflects advection (*AD*) and a contribution proportional to diabatic heating (Q) gradients here termed *DH*:

$$\frac{\partial PV}{\partial t} \equiv PVT \approx AD + DH,$$

where $DH = \rho^{-1}\left[(f+\zeta)\frac{\partial Q}{\partial z} + \left(\frac{\partial u}{\partial z} - \frac{\partial w}{\partial x}\right)\frac{\partial Q}{\partial y} + \left(\frac{\partial w}{\partial y} - \frac{\partial v}{\partial z}\right)\frac{\partial Q}{\partial x}\right]$, ρ is density, f is the Coriolis parameter, and ζ is the vertical component of relative vorticity. In cyclonic vortices, PV is created where Q increases with height, and thus differences in the magnitude, distribution and vertical structure of diabatic heating around the storm can influence motion. WW noted that *AD* incorporates the indirect response to heating in addition to the beta drift and extracted the azimuthal wavenumber 1 components of these terms. We computed the more general asymmetric fields (Figure 3), focusing on the 2–3.5 km layer to avoid surface friction and significant radiative effects, and estimated contributions to the storm motion vector C using least squares, as by WW.

[13] Among these cases, the K storm (Figure 3a) may best represent the beta effect in isolation, as its largely symmetric updraft (Figure 2a) resulted in little diabatic contribution to asymmetric PV. Note the C and *AD* vectors nearly align and indicate rapid northwestern motion. For the other storms, *DH* is greater and its correlation with *AD* is significant and negative, making storm motion the small difference between large, opposing terms. The net motion might also be interpreted as a competition between the generally northwestward-directed beta drift incorporated in *AD* and the diabatic heating, with storm direction determined by their relative orientations and magnitudes. For the S_2 (Figure 3b) case, *DH* points southeastward, directly opposing the expected drift. Thus, it appears that asymmetric diabatic heating was primarily acting to slow the storm motion in this case, which progressed at roughly half the speed of the K storm.

[14] For the L storm with CRF active (Figure 3c), *DH* is further rotated counterclockwise relative to the S_2 case, ostensibly encouraging a more northerly net movement. The stronger and more concentrated updraft of the CRF-off L* vortex apparently led to diabatic heating having more influence on motion. With the heating rotated to the eastern flank, the advection term is shifted to the west side, such that the two vectors remain largely in opposition. The combination of northwestward-directed beta and eastward-pointing *DH* appears to have imparted a motion that is slightly east of north in this case.

4. Sensitivity to Absorption Coefficients

[15] How and why CRF influences storm dynamics, thermodynamics and structure is not completely understood. Moreover, this motivates a closer examination of how cloud-radiative feedback is implemented and its associated sensitivities. An initial investigation focuses on the LW component, which appears to be a primary driver. WRF's RRTM scheme presently follows *Dudhia* [1989] and gives cloud droplets and ice crystals fixed absorption coefficients of $\alpha_c = 0.144$ and $\alpha_i = 0.0735$ m^2 g^{-1}, respectively. These are used to compute optical path lengths and altering them influences the magnitude and altitude at which LW cooling and heating take place. For rain and snow, the coefficients vary with concentration (although are not optimally tied to

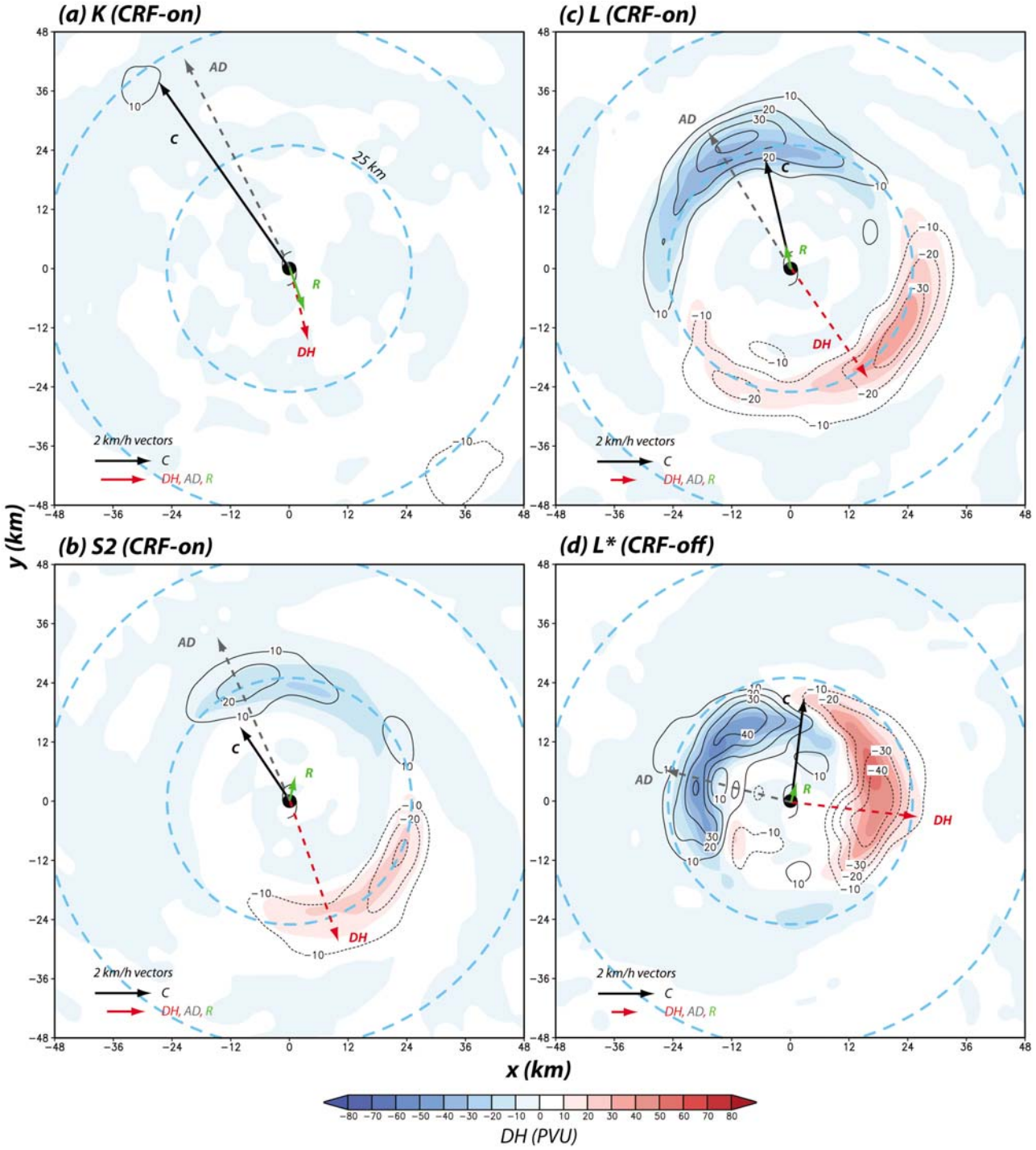

Figure 3. Asymmetric components of *AD* (contoured) and *DH* (shaded) for cases (a) K, (b) S_2, (c) L and (d) L*, averaged through the 2–3.5 km layer in a 96 km square region over the final 24 h, with storm motion vector *C*. Vectors *AD* and *DH* were obtained using least squares minimization and the residual vector $R = C - AD - DH$ represents missing terms and other errors. Similar motion vectors obtained from *PVT* are not shown.

the MP schemes, especially the more sophisticated ones), and graupel mass is neglected. For a 1 kg m^{-3} mass content, the snow (α_s = 2.34E-3) and rain (α_r = 0.33E-3 m^2 g^{-1}) absorption coefficients are 3.2 and 0.5% of α_i, respectively.

[16] One aspect that varies among MP schemes is the quantity and species apportionment of condensate, and this could produce different radiative sensitivities. For cases W6ˆ and S_2ˆ (Figure 4), the LW radiative impact of snow was neglected (i.e., α_s = 0), as is done in some versions of RRTM and in the German Weather Service COSMO model. Storm W6ˆ eventually tracked to the east of its unmodified counterpart, due in part to variations that occurred early in the simulation, while the S_2ˆ path was virtually identical to its control. The unmodified S_2 produced little snow beyond 100 km from the center, at least compared to W6 (Figure 4a, inset), which may be why neglecting snow had little effect.

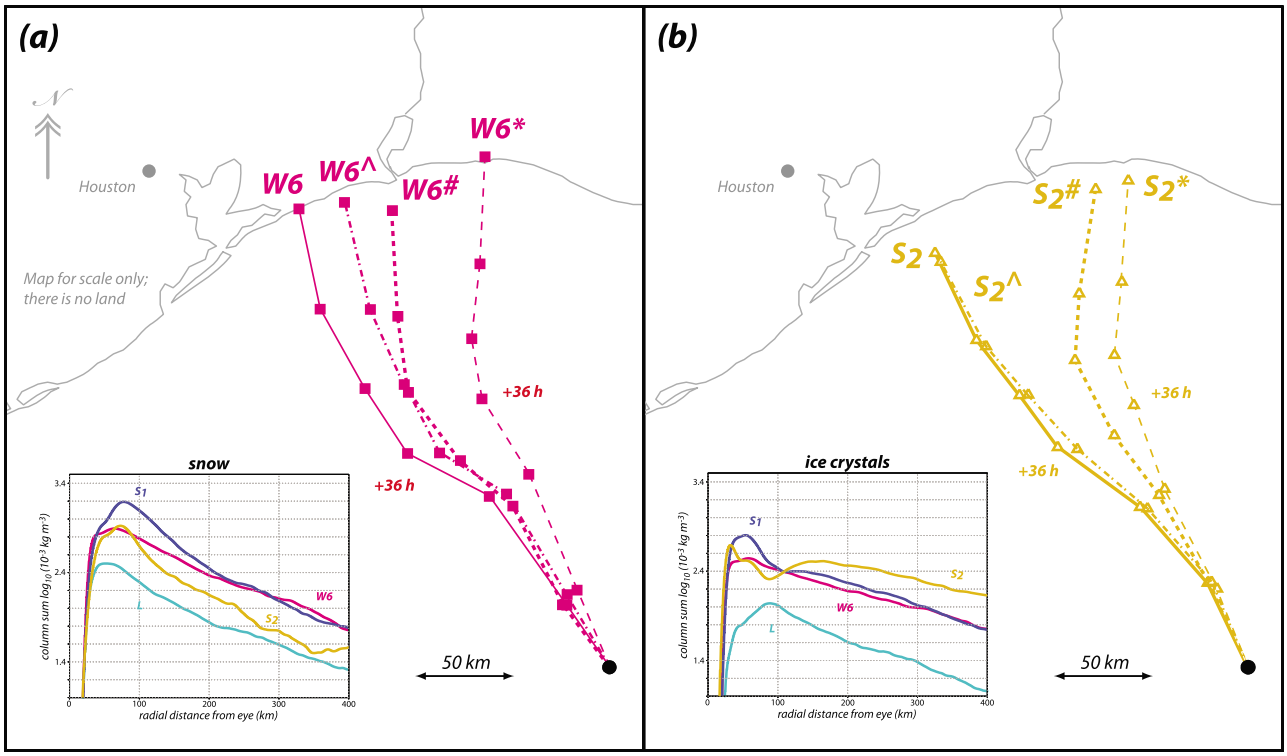

Figure 4. As in Figure 1 except for schemes W6 and S_2 that demonstrate absorption coefficient sensitivity. Insets show radial profiles of column total (a) snow and (b) ice and represent time-averaged symmetric components; vertical axis is $\log_{10}$ scaled.

[17] For cases $W6^{\#}$ and $S_2^{\#}$, $\alpha_i = \alpha_s$. Although investigated merely as a test, this is tantamount to making ice particles denser or apportioning the mass among fewer, larger particles; both effects diminish the species' ability to interact with LW radiation. The impact on both storm tracks is substantially greater. The $W6^{\#}$ storm moved in a northerly direction after 48 h, which is more similar to the original L cyclone, while case $S_2^{\#}$ tracked parallel to its CRF-off version. The larger S_2 response may reflect the fact that this MP produced more ice beyond the core than the other unmodified runs (Figure 4b, inset). Unlike the other cases, there is more ice than snow in S_2 for radius $r \geq 120$ km.

[18] Finally, it is suggested that the uniqueness of the K scheme results from its areally extensive concentrations of cloud water, which has a very large radiative impact. As pointed out in Paper 2, K storms tend to support large, thick anvils owing to the lack of mechanisms for producing precipitation-sized particles from cloud droplets when concentrations are too low to activate autoconversion. In contrast, all of the ice-containing schemes can transfer condensate to fast-falling graupel, which is routinely presumed not to influence radiation. Again, the pressing question is why CRF has acted to alter storm structure and strength. At least in these simulations, including CRF always resulted in the storms becoming less intense with respect to vertical motions and maximum horizontal winds.

5. Summary

[19] Idealized simulations have demonstrated that cloud microphysical assumptions can influence TC motion and track forecasts, and here cloud-radiative feedback is shown to play a major role in this sensitivity. Vortex motion reflects a competition between beta drift and convective heating variations responding in part to beta-induced asymmetries. Beyond modulating the symmetric components of storm structure (Paper 2), MP schemes generated different heating patterns that apparently contribute to subtle but important track changes. When CRF was neglected, however, the convective asymmetries were not only more significant but also largely independent of the MP. For some reason, CRF appeared to act through MPs to weaken and/or "smear" out the diabatic effects in ways and degrees that were scheme-dependent. These MPs produce different amounts, types and distributions of particles they produce, and ostensibly impact storm dynamics or thermodynamics through LW absorption and emission. Idealized studies often neglect CRF, which may explain why MP sensitivity is not always encountered.

[20] Future work will employ advanced radiation parameterizations that are more tightly linked to the MPs, and reconsider cyclone initialization. Although each simulation began with a coherent TC with tropical storm intensity, considerable further development occurred in the first 36 h or so, which may have delayed and possibly limited structure and track differentiation. This intensification phase is of practical importance, as many models often start with TCs having structures and intensities different than what the model physics, resolution and environmental conditions can and will eventually support. That said, this study highlights the value of further consideration of cloud-radiative feedbacks in idealized and operational contexts.

[21] **Acknowledgments.** This work was supported by NSF grant ATM-0554765, the Jet Propulsion Laboratory SURP program and The Aerospace Corporation.

References

Bender, M. A. (1997), The effect of relative flow on the asymmetric structure in the interior of hurricanes, *J. Atmos. Sci.*, *54*, 703–724.

Chan, J. C.-L., and R. T. Williams (1987), Analytical and numerical studies of the beta-effect in tropical cyclone motion, *J. Atmos. Sci.*, *44*, 1257–1265.

Corbosiero, K. L., and J. Molinari (2002), The effects of vertical wind shear on the distribution of convection in tropical cyclones, *Mon. Weather Rev.*, *130*, 2110–2123.

Dudhia, J. (1989), Numerical study of convection observed during the Winter Monsoon Experiment using a mesoscale two-dimensional model, *J. Atmos. Sci.*, *46*, 3077–3107.

Dunion, J. P., and C. S. Marron (2008), A reexamination of the Jordan mean tropical sounding based on awareness of the Saharan air layer: Results from 2002, *J. Clim.*, *21*, 5242–5253.

Fiorino, M. J., and R. L. Elsberry (1989), Some aspects of vortex structure related to tropical cyclone motion, *J. Atmos. Sci.*, *46*, 975–990.

Fovell, R. G., and H. Su (2007), Impact of cloud microphysics on hurricane track forecasts, *Geophys. Res. Lett.*, *34*, L24810, doi:10.1029/2007GL031723.

Fovell, R. G., K. L. Corbosiero, and H.-C. Kuo (2009), Cloud microphysics impact on hurricane track as revealed in idealized experiments, *J. Atmos. Sci.*, *66*, 1764–1778.

Frank, W. M., and E. A. Ritchie (1999), Effects of environmental flow upon tropical cyclone structure, *Mon. Weather Rev.*, *127*, 2044–2061.

Holland, G. J. (1983), Tropical cyclone motion: Environmental interaction plus a beta effect, *J. Atmos. Sci.*, *40*, 328–342.

Jordan, C. L. (1958), Mean soundings for the West Indies area, *J. Meteorol.*, *15*, 91–97.

Seifert, A., and K. D. Beheng (2006), A two-moment cloud microphysics parameterization for mixed-phase clouds. Part I: Model description, Meteorol. *Atmos. Phys.*, *92*, 45–66.

Wang, Y. (2009), How do outer spiral rainbands affect tropical cyclone structure and intensity?, *J. Atmos. Sci.*, *66*, 1250–1273.

Wu, L., and B. Wang (2000), A potential vorticity tendency diagnostic approach for tropical cyclone motion, *Mon. Weather Rev.*, *128*, 1899–1911.

Wu, L., and B. Wang (2001), Effects of convective heating on movement and vertical coupling of tropical cyclones: A numerical study, *J. Atmos. Sci.*, *58*, 3639–3649.

K. L. Corbosiero, R. G. Fovell, and K.-N. Liou, Department of Atmospheric and Oceanic Sciences, University of California, 405 Hilgard Ave., Los Angeles, CA 91361-1565, USA. (kristen@atmos.ucla.edu; rfovell@ucla.edu; knliou@atmos.ucla.edu)

A. Seifert, German Weather Service, Frankfurterstr. 135, D-63067 Offenbach, Germany. (axel.seifert@dwd.de)